

Long baseline neutrino experiments, mass hierarchy and δ_{CP}

C. R. Das^{*}, João Pulido[†]

CENTRO DE FÍSICA TEÓRICA DE PARTÍCULAS (CFTP)

Departamento de Física, Instituto Superior Técnico

Av. Rovisco Pais, P-1049-001 Lisboa, Portugal

Abstract

We investigate the possibilities offered by the long baseline experiments T2K, *Nova*, LBNE and LAGUNA for the evaluation of the neutrino mass hierarchy and CP violating phase δ_{CP} . We consider a neutrino and antineutrino energy in the interval $[0.5, 12]$ GeV. It is found that the clearest possible distinction between the two hierarchy signatures is provided by LAGUNA for an (anti)neutrino energy $E_{(\bar{\nu})\nu} \simeq 0.5$ GeV in the $(\bar{\nu}_\mu \rightarrow \bar{\nu}_\mu)$ $\nu_\mu \rightarrow \nu_\mu$ disappearance channel. For LBNE at $E_{\bar{\nu}} \simeq 1$ GeV the $\bar{\nu}_\mu \rightarrow \bar{\nu}_\mu$ channel may also provide a distinction, although not so clear, and for *Nova* this may be even less clear. These results are essentially the same for the θ_{23} first and second octant solutions. As for δ_{CP} determination, LAGUNA also offers the best chances at $E_{\bar{\nu}} \simeq 0.5$ GeV in the $\bar{\nu}_\mu \rightarrow \bar{\nu}_e$ channel with θ_{23} in either octant. Regarding nonstandard interactions, the best possibility for their investigation resides in *Nova* whose source-far detector distance can become a magic baseline if the hierarchy is normal for channels $\nu_\mu \rightarrow \nu_\mu$, $\bar{\nu}_\mu \rightarrow \bar{\nu}_e$, $\bar{\nu}_\mu \rightarrow \bar{\nu}_\mu$ with energy (8.9-9.1) GeV, (11.6-12) GeV, (8.8-12) GeV. If the hierarchy is inverse, magic baselines for *Nova* occur for $\nu_\mu \rightarrow \nu_e$, $\nu_\mu \rightarrow \nu_\mu$, and $\bar{\nu}_\mu \rightarrow \bar{\nu}_\mu$ with energy (11.8-12) GeV, (8.9-12.3) GeV, (8.8-8.9) GeV. For LAGUNA a magic baseline appears for the $\bar{\nu}_\mu \rightarrow \bar{\nu}_\mu$ channel only at (4.7-5.0) GeV in inverse hierarchy. We have also investigated a possible complementarity between T2K and *Nova*.

^{*}E-mail: crdas@cftp.ist.utl.pt

[†]E-mail: pulido@cftp.ist.utl.pt

1 Introduction

The solar and atmospheric neutrino anomalies [1] - [8] have since long ago motivated interest [9] in long baseline (LBL) neutrino experiments ([10] - [14]), aiming at an accurate evaluation of some of the neutrino parameters [‡]. Among these, the values of the mass squared differences and mixing angles are by now reasonably well established from the data of the solar [1] - [7], atmospheric [8] and reactor experiments [16] - [18]. Still, several issues on neutrino parameters are still open, namely the absolute mass, the mass hierarchy and the magnitude of δ_{CP} , the CP violating phase. LBL neutrino experiments, either from accelerators [11] - [14], [19], neutrino factories or beta beams [20], [21] will be essential in providing the answer to the two most important questions, namely, whether the hierarchy is normal (NH, $\Delta m_{31}^2 > 0$) or inverse (IH, $\Delta m_{31}^2 < 0$) and whether or not CP violation occurs in the leptonic sector ($\sin \delta_{CP} \neq 0$).

The recent measurement of the θ_{13} mixing angle [16], [18] reduces the parameter degeneracy [22] - [25] inherent in the LBL three neutrino analysis, so that the above goals have become within reach of the forthcoming experiments. Besides the existing T2K [12] and *No ν a* [13], the latter expected to start taking data soon, two other major projects are being considered: LBNE [19] and LAGUNA/LBNO [26]. The first, whose proposal is under current evaluation, aims at sending a neutrino beam from Fermilab to Homestake (~ 1290 km) and the second favours a baseline from CERN to the Pyhasälmi mine in Finland (~ 2290 km) with a proposal expected to be submitted by 2014 [26].

The present generation of LBL neutrino experiments [11] - [14] relies on high energy neutrino beam facilities where charged pions and kaons are allowed to decay in flight. The neutrino (antineutrino) beam composition consists mostly of muon neutrinos (antineutrinos) with a small mixture of electron neutrinos (antineutrinos) and a small component of tau neutrinos if the beam energy is high enough. An alternative to obtain neutrino beams for LBL experiments has been proposed some time ago based on muon storage rings [28], [29] whereby muons produced from meson decays are stored, accelerated and allowed to decay in the long straight sections of a storage ring [30]. These sections are aligned in the direction of the neutrino detectors which can be located several thousands of kilometers away. Since muons and antimuons decay to almost 100% according to

$$\mu^- \rightarrow e^- \bar{\nu}_e \nu_\mu, \quad \mu^+ \rightarrow e^+ \nu_e \bar{\nu}_\mu,$$

the precise content of the neutrino and antineutrino beam can be accurately determined.

There have been many studies of CP symmetries and mass hierarchy via neutrino oscillations for present and future facilities (see e.g. [31] - [36]) and the prospects for their determination have considerably improved after the measurement of θ_{13} [16], [18]. In the present work we take advantage of this fact and explore the possibility for extracting δ_{CP} and the mass hierarchy from the T2K [12], *No ν a* [13], LBNE [19] and LAGUNA/LBNO [26]

[‡]For a recent review on LBL neutrino experiments see [15].

LBL neutrino experiments. As shall be seen, by conveniently choosing a neutrino energy range and source-detector distance, the parameter degeneracy involving the mass hierarchy and δ_{CP} can be overcome with the data from a single experiment. In fact to this end one detector located sufficiently far away from the source may be enough, as already noted in [37]. Of course the possible redundancy provided by one or two extra detectors will always be welcome for the verification and accuracy of the results [§].

This paper is organized as follows: we start in section 2 with the derivation of the general expression for the oscillation probability in matter with constant density without resorting to any approximations. In section 3 we start by comparing the results of our numerical calculation with the leading term approximations used in the literature [39], [40], [41]. From the oscillation probability expression we obtain the biprobability plots [39] for a few relevant pairs of oscillation channels in which most of our analysis will be based. Thus in subsection 3.1 we get such plots for fixed distance, varying energy and several values of δ_{CP} , in the cases of normal and inverse hierarchies. It will be seen that within preferred energy ranges the relative ordering of the iso- δ_{CP} curves remains invariant as the energy changes, while for other energy regions at the same distance they successively intersect each other. In these cases, for a small change in energy any two neighbouring curves may swap their relative position. This entails a less accurate, if at all possible, determination of δ_{CP} in the corresponding energy range at that distance. In fact the biprobability curves for constant energy as a function of δ_{CP} are closed contours which intersect the iso- δ_{CP} curves. Since the neutrino energy cannot be known with arbitrarily good accuracy, the two parameters (beam energy and distance from source) must be conveniently chosen to ensure that the iso- δ_{CP} curves do not intersect each other within the energy uncertainty range. Moreover the regions of sudden variations of the CP phase along the closed contours should be avoided so that δ_{CP} could be determined with a reasonable accuracy. In subsection 3.2 we obtain the biprobabilities for fixed energy, varying distance and several values of δ_{CP} also for both hierarchies. Closed contours are now obtained for constant distances as a function of the CP phase and the same rule as before applies for the requirement of its accurate determination. Thus far our analysis will only use the first octant solution for the θ_{23} mixing angle and is mainly focused on the *No ν a*, LBNE and LAGUNA experiments. It turns out that the latter experiment appears to be particularly promising as regards its contribution to providing definite conclusions for the mass hierarchy and the δ_{CP} range. At the end of section 3.2 we provide a comparison between the θ_{23} first and second octant solutions in the three experiments. Section 4 is dedicated to a comparison of T2K and *No ν a* emphasizing the prospective distinction in these experiments between the signatures of mass hierarchies and between the signatures of the first and second octant solutions for θ_{23} . Finally in section 5 we summarize the present work and draw our conclusions.

[§]The idea of two detectors placed at different baselines was first proposed in [38]. However, owing to the limited knowledge on the mass differences and mixing angles at the time, a solution to the degeneracies was far from reachable.

2 The oscillation probability

The starting point for our neutrino oscillation analysis is the standard matter Hamiltonian which in the flavour basis reads

$$H^{(f)} = U \begin{pmatrix} 0 & 0 & 0 \\ 0 & \frac{\Delta m_{21}^2}{2E} & 0 \\ 0 & 0 & \frac{\Delta m_{31}^2}{2E} \end{pmatrix} U^\dagger + \begin{pmatrix} V_k & 0 & 0 \\ 0 & 0 & 0 \\ 0 & 0 & 0 \end{pmatrix} \quad (1)$$

where $\Delta m_{ji}^2 = m_j^2 - m_i^2$, $V_k = \sqrt{2}G_F N_{ek}$, G_F is the Fermi constant and N_{ek} is the electron density in the k^{th} layer. The latter can be expressed in terms of the mass density ρ_k , the electron number density Y_k and the nucleon mass m_N as

$$N_{ek} = \frac{Y_k \rho_k}{m_N}. \quad (2)$$

For the cases we study we need only to consider propagation within the Earth's crust, for which $\rho_k = 3 \text{ g cm}^{-3}$ and $Y_k = 1/2$. In eq.(1) U is the usual leptonic mixing matrix $PMNS$ relating the neutrino mass basis to the flavour basis[¶]

$$|\nu_\alpha\rangle = U|\nu_i\rangle \quad (3)$$

and in a like manner for future purpose one can define a unitary transformation relating the mass matter eigenstates to the flavour ones

$$|\nu_\alpha\rangle = U'|\nu'_i\rangle. \quad (4)$$

Given the definition of U (eq.(3)), denoting by $H^{(m)}$ the mass basis Hamiltonian operating between mass eigenstates $|\nu_i\rangle$ and $\langle \nu_j|$ and $H^{(f)}$ the flavour basis one operating between flavour eigenstates $|\nu_\alpha\rangle$ and $\langle \nu_\beta|$, we have

$$\langle \nu_j|H^{(m)}|\nu_i\rangle = \langle \nu_\beta|UH^{(m)}U^\dagger|\nu_\alpha\rangle = \langle \nu_\beta|H^{(f)}|\nu_\alpha\rangle \quad (5)$$

hence

$$H^{(f)} = UH^{(m)}U^\dagger. \quad (6)$$

Since $H^{(f)}$ and $H^{(m)}$ are related by a unitary transformation their eigenvalues are the same, therefore denoting by V_f and V respectively the matrices that diagonalize $H^{(f)}$ and $H^{(m)}$

$$V_f^\dagger H^{(f)} V_f = V^\dagger H^{(m)} V = H_D \quad (7)$$

where H_D is the diagonalized Hamiltonian. Using (6) one obtains the relation between matrices V_f and V ,

$$V_f = UV \quad (8)$$

[¶]We use the Particle Data Group notation [42] for the U matrix.

so that UV also diagonalizes the flavour basis Hamiltonian as can be easily checked from eqs.(1) and (6). Moreover applying the definition of U' (eq.(4))

$$\langle \nu_\beta | H^{(f)} | \nu_\alpha \rangle = \langle \nu'_j | (U')^\dagger H^{(f)} U' | \nu'_i \rangle \quad (9)$$

which shows that U' also diagonalizes H^f , thus $U' = V_f = UV$.

Since the neutrino Hamiltonian (1) satisfies a Schrödinger like equation

$$i \frac{d}{dx} \nu_\alpha = H_{\alpha\beta}^{(f)} \nu_\beta \quad (\alpha, \beta = e, \mu, \tau) , \quad (10)$$

a state produced as flavour α at the origin becomes, after traveling a distance L

$$\nu_\beta(L) = S_{\beta\alpha}(L, 0) \nu_\alpha(0) \quad (11)$$

where $S_{\beta\alpha}(L, 0)$ satisfies the same Schrödinger equation. So in index notation

$$S_{\beta\alpha}(L, 0) = (U')_{\beta i} \exp \left[-i \int_0^L (U'^*)_{\gamma i} (H^{(f)})_{\gamma\delta} (U')_{\delta j} dx \right] (U'^*)_{\alpha i} = (U')_{\beta i} e^{-i\lambda_i L} (U'^*)_{\alpha i} \quad (12)$$

where λ_i 's are the mass matter eigenvalues. The oscillation probability

$$P(\nu_\alpha \rightarrow \nu_\beta, L) = |S_{\beta\alpha}|^2 \quad (13)$$

is then evaluated through

$$P(\nu_\alpha \rightarrow \nu_\beta, L) = (U'^*)_{\beta i} e^{i\lambda_i L} (U')_{\alpha i} (U')_{\beta j} e^{-i\lambda_j L} (U'^*)_{\alpha j} \quad (\text{no sum in } \alpha, \beta) \quad (14)$$

with the following neutrino parameter values [43],

$$\begin{aligned} \sin^2 \theta_{12} &= 0.31, \quad \sin^2 \theta_{13} = 2.4 \times 10^{-2}, \quad \sin^2 \theta_{23} = 0.39, \\ \Delta m_{21}^2 &= 7.6 \times 10^{-5} eV^2, \quad \Delta m_{31}^2 = 2.4 \times 10^{-3} eV^2. \end{aligned} \quad (15)$$

For the sake of comparison we will present one example with the second octant solution for θ_{23} [44]

$$\sin^2 \theta_{23} = 0.61. \quad (16)$$

We will use equation (14) throughout the paper as the basis for our calculations.

3 $\text{No}\nu\text{a}$, LBNE, LAGUNA

The channels to analyse in this section are the ones for which the three experiments ($\text{No}\nu\text{a}$, LBNE and LAGUNA) are dedicated, namely the muon neutrino disappearance channel ($\nu_\mu \rightarrow \nu_\mu$), the inverse golden channel or electron neutrino appearance ($\nu_\mu \rightarrow \nu_e$) and their antineutrino counterparts for normal and inverse hierarchy. We denote these channels as $\mu\mu$,

μe , their counterparts as $\bar{\mu}\bar{\mu}$, $\bar{\mu}\bar{e}$ respectively and accordingly their oscillation probabilities as $P_{\mu\mu}, P_{\mu e}, P_{\bar{\mu}\bar{\mu}}, P_{\bar{\mu}\bar{e}}$. As mentioned in the introduction our main results are presented in terms of biprobability graphs.

In the current literature the oscillation probabilities for long baselines are usually calculated by resorting to approximations up to first or second order in 'small' parameters such as [27], [39], [40], [41], [46]

$$\frac{2\sqrt{2}G_F N_e E}{\Delta m_{31}^2}, \frac{\Delta m_{21}^2}{2E} L, \frac{\Delta m_{21}^2}{\Delta m_{31}^2}, \theta_{13}, \frac{\Delta m_{21}^2}{\Delta m_{31}^2} = \epsilon \simeq \theta_{13}.$$

In particular, as it is known nowadays, the approximation $\epsilon \simeq \theta_{13}$ is rather inaccurate. Here we will use instead the exact numerical expressions from (14) and show in fig.1 the comparison between our results and those from the approximations used in the literature. In the four top panels of fig.1 we plot the oscillation probability $P_{\mu e}$ as a function of distance for eight values of δ_{CP} equally spaced from 0 to 360 degrees and in the two bottom panels the biprobability plots for the channel pair $\mu e, \bar{\mu}\bar{e}$. Here we consider normal hierarchy only and a neutrino energy $E=2.3$ GeV. Notice the large discrepancies in the probabilities and the locations of the intersections from panel to panel. These intersections correspond to the magic baselines to which we will return in section 3.2.

3.1 Fixed distance biprobability plots

In this subsection we just consider the *Nova* [13] and LBNE [19] experiments and study the constant δ_{CP} curves as a function of energy for fixed distance.

Nova is planned to start taking data in 2013 and consists of a 330 ton near detector at the Fermilab site and a 14 kiloton far detector. The latter is a liquid scintillator situated 12 km off-axis at 810 km in the Neutrino Main Injector (NuMI) beam produced at Fermilab. It is dedicated mainly to observe $\nu_\mu \rightarrow \nu_e$ oscillation along with its antiparticle counterpart. The advantage of an off-axis location is that the neutrino energy is nearly independent from the parent meson energy, therefore the beam energy spread is much smaller than for an on-axis one [45]. Also using the NuMI beam, but not yet finally approved, is LBNE with a 34 kton liquid Argon far detector at 1290 km distance and a neutrino energy in the interval [0.5,12] GeV.

In each of the four panels of fig.2 we show the biprobability curves for the pair of channels $\mu e, \mu\mu$ for eight values of δ_{CP} equally spaced from 0 to 360 degrees with energy running from 0.5 GeV to 100 GeV. The top two panels refer to a distance of 810 km and the bottom two are for 1290 km which are the source-far detector distances for *Nova* and LBNE respectively. The left panels are for normal and the right ones are for inverse hierarchy. In each panel we plot the biprobability curves for three energies which are ellipses of large eccentricity: for 810 km we take $E=2.3$ GeV which is the preferred *Nova* energy (middle ellipses in the top panels), $E=1$ GeV and 0.5 GeV (top and bottom ellipses respectively). In order to keep the figures as clear as possible, we choose not to continue the iso- δ_{CP} curves for $E<1$ GeV.

The most favourable energy range for the evaluation of δ_{CP} is the one where the iso- δ_{CP} curves lie the furthest apart since the phase variation is then the smoothest possible along each ellipse. Consequently, as it is seen from all four panels of fig.2, a value near $E=0.5$ GeV is the best choice for δ_{CP} evaluation. For 1290 km (LBNE source-detector distance) we take $E=7$ GeV, 1 GeV and 0.5 GeV (top, middle and bottom ellipses in the bottom panels of fig.2). Again we omit the iso- δ_{CP} curves below 1 GeV and find that the best sensitivity to δ_{CP} is for 0.5 GeV, although a double degeneracy remains in its determination due to the very large eccentricity of the ellipses. In the limit of increasing energies the constant δ_{CP} curves merge and eventually coincide at the point $(P_{\mu e} = 0, P_{\mu\mu} = 1)$ whereas they diverge from each other for decreasing energy. This is consistent with the fact that the oscillation length increases for increasing energy, so for fixed distance the neutrinos oscillate less as their energy increases. The same as in fig.2 is done in figs.3 and 4 for the pairs of channels $\bar{\mu}\bar{e}$, $\bar{\mu}\bar{\mu}$ and μe , $\bar{\mu}\bar{e}$ respectively. In fig.3 (for $\bar{\mu}\bar{e}$, $\bar{\mu}\bar{\mu}$) and in the top panels, the middle ellipses are for $E=2.3$ GeV, the top and bottom ones for $E=1$ GeV and 0.5 GeV respectively, all for 810 km distance as in fig.2. In the bottom panels (1290 km) the top, middle and bottom ellipses are for $E=7$ GeV, 1 GeV and 0.5 GeV. Once again the iso- δ_{CP} curves are omitted below 1 GeV while 0.5 GeV is the most convenient choice as regards δ_{CP} evaluation, if not for a double degeneracy. As for the channel pair μe , $\bar{\mu}\bar{e}$ (fig.4) the 0.5 GeV contours are again the ellipses with the longest major axes. So this energy is also the most convenient choice for δ_{CP} evaluation. It will be seen in the next section that an improved situation can be found with data from LAGUNA.

The possibility of distinction between hierarchies appears realistic so long as the neutrino energy can be appropriately tuned, as can be inferred from the comparison between the two bottom panels of fig.3 ($\bar{\mu}\bar{e}$, $\bar{\mu}\bar{\mu}$ channels at the LBNE source-detector distance). In fact for $E=1$ GeV, which corresponds to the middle ellipse, it is seen that $P_{\bar{\mu}\bar{\mu}} \simeq 0.48$ for inverse hierarchy whereas for normal hierarchy $0.62 \lesssim P_{\bar{\mu}\bar{\mu}} \lesssim 0.66$. Not so clear a distinction can be provided at the *Nova* distance for the same energy, as one can conclude from the comparison between the two top panels in figs.2 and 3.

In a like manner as figs.2, 3, 4, fig.5 shows the biprobability curves for the $\mu\mu$, $\bar{\mu}\bar{\mu}$ channel pair in normal hierarchy for 0.5 GeV, 1 GeV and 2.3 GeV at 810 km. In this case the iso- δ_{CP} curves are nearly superimposed, so that an unrealistically large experimental accuracy would be needed in order to obtain information on δ_{CP} . The same situation occurs for inverse hierarchy for the same energies and distance and for normal and inverse hierarchies at 1290 km with 0.5 GeV, 1 GeV and 7 GeV. Hence the $\mu\mu$, $\bar{\mu}\bar{\mu}$ channel combination is of little use, if any.

3.2 Fixed energy biprobability plots

In this subsection we extend our analysis to include the LAGUNA experiment and study the constant δ_{CP} curves as a function of distance for fixed neutrino energy from the production point up to 2290 km. This is the CERN-Pyhasälmä mine distance where the LAGUNA

detector is planned to be installed observing neutrinos produced from CERN. We consider two neutrino energies: $E=2.3$ GeV and 0.5 GeV. Our results are plotted in figs.6, 7 (for 2.3 GeV) and 8, 9 (for 0.5 GeV). The top panels in fig.6 contain the biprobability curves for the μe , $\mu\mu$ channel pair, the middle ones for $\bar{\mu}\bar{e}$, $\bar{\mu}\bar{\mu}$ and the bottom ones for μe , $\bar{\mu}\bar{e}$. Left hand panels are for normal and right hand ones for inverse hierarchy respectively. The iso- δ_{CP} curves are shown for eight values of δ_{CP} equally spaced from 0° to 360° as a function of distance, all diverging from a common point at zero distance. The constant distance contours are for 810 km (Nova, dotted lines), 1290 km (LBNE, dashed lines) and 2290 km (LAGUNA, full lines).^{||} Note that the Nova and LBNE contours correspond to the ones already shown in fig.2 for μe , $\mu\mu$ now superimposed on the iso- δ_{CP} curves for varying energy instead of varying distance as before. In the top right and middle left panels of fig.6 (μe , $\mu\mu$ channel pair, inverse hierarchy and $\bar{\mu}\bar{e}$, $\bar{\mu}\bar{\mu}$ channel pair, normal hierarchy) all curves intersect at one point. This corresponds to one of the channel probabilities being independent of δ_{CP} at one particular distance, the so called magic baseline. Such distance can be evaluated by expanding the appearance probability

$$P_{\mu e} = |(U')_{ei}e^{-i\lambda_i L}(U'^*)_{\mu i}|^2 \quad (17)$$

and separating the δ_{CP} dependent and independent terms. We obtain

$$P_{\mu e} = 2s_{12}c_{12}s_{23}c_{23}s_{13}c_{13}^2(A s_\delta + B c_\delta) + \delta_{CP} \text{ independent terms} \quad (18)$$

with

$$\begin{aligned} A &= \sin(\lambda_1 - \lambda_2)L - \sin(\lambda_1 - \lambda_3)L + \sin(\lambda_2 - \lambda_3)L \\ B &= c_{2\theta_{12}}[1 - \cos(\lambda_1 - \lambda_2)L] - \cos(\lambda_1 - \lambda_3)L + \cos(\lambda_2 - \lambda_3)L \end{aligned} \quad (19)$$

where $c_{12} = \cos\theta_{12}, \dots$ and L is the distance from the source to the detector. In order to ensure the independence of $P_{\mu e}$ on δ_{CP} one must require the vanishing of the quantity in brackets in (18). To this end we note that the three arguments of the sines and cosines in the expressions for A and B cannot simultaneously vanish for any possible baseline distance and moreover such condition would only be a sufficient one for $P_{\mu e}$ to become independent of δ_{CP} . So one must impose

$$\tan \delta_{CP} = -\frac{B}{A} \quad (20)$$

for any δ_{CP} , which requires $A = B = 0$. In this way for $E=2.3$ GeV one gets for the first three magic baselines for the μe channel in inverse hierarchy $L_{magic} \simeq 1980$ km, $\simeq 3960$ km and $\simeq 5940$ km (see fig.7). Hence the common point of all curves in the top right panel of fig.6 corresponds to the shortest one at 1980 km. Analogously, for the $\bar{\mu}\bar{e}$, $\bar{\mu}\bar{\mu}$ channel pair in normal hierarchy, the magic baselines occur for $\bar{\mu}\bar{e}$, the shortest one being located at

^{||}The preferred neutrino energy for LAGUNA has not been decided yet. Here we consider the same energies for all three experiments so that the corresponding closed contours appear in the same panel.

$L_{magic} \simeq 2008 \text{ km}$, and the following ones at approximately 4020 km and 6030 km . They can be easily determined in the same way as in the previous case with the replacements

$$U' \rightarrow U'^* \quad V \rightarrow -V. \quad (21)$$

Magic baselines are particularly useful for the investigation of nonstandard interactions [46], [47], [48].

Fig.8 shows the biprobability contours for a neutrino energy $E=0.5 \text{ GeV}$ and the same channels as fig.6 at the *No ν a* (dotted), LBNE (dashed) and LAGUNA (full) distances. For simplicity the iso- δ_{CP} curves are omitted from fig.8.

From the inspection of figs.6 and 8 (neutrino energies 2.3 GeV and 0.5 GeV respectively) one can infer the prospects for distinguishing between normal and inverse hierarchies. To this end one must compare the left and right panels of these figures. Starting with fig.6 (middle panels) it is seen that for LBNE alone (bottom ellipse appearing as a line segment) normal hierarchy gives $0.012 \lesssim P_{\bar{\mu}e} \lesssim 0.034$, $P_{\bar{\mu}\bar{\mu}} \sim 0.06$ while inverse hierarchy gives $0.042 \lesssim P_{\bar{\mu}e} \lesssim 0.078$, $P_{\bar{\mu}\bar{\mu}} \sim 0.09$. Also for LBNE and appearance probabilities only, the comparison of the bottom panels of fig.6 shows for normal hierarchy $0.042 \lesssim P_{\mu e} \lesssim 0.078$, $0.012 \lesssim P_{\bar{\mu}e} \lesssim 0.034$ while for inverse hierarchy such probabilities are interchanged. Another typical case can be observed from the top panels of fig.6 with the uppermost ellipses which correspond to the LAGUNA experiment. Here it is seen that $0.012 \lesssim P_{\mu e} \lesssim 0.060$ and $P_{\mu e} \lesssim 0.020$ for normal and inverse hierarchy respectively, hence some overlap exists in the two probabilities. As for the $\mu\mu$ channel one has $0.91 \lesssim P_{\mu\mu} \simeq 0.95$ and $0.97 \lesssim P_{\mu\mu} \lesssim 1$ for normal and inverse hierarchies, a difference which will be difficult to detect experimentally. A similar conclusion may be drawn from the inspection of the remainder of fig.6. Therefore the distinction between the two hierarchies appears to be too difficult to trace with a neutrino energy 2.3 GeV .

In contrast, for $E=0.5 \text{ GeV}$ the distinction between signatures from each hierarchy becomes much more plausible especially with the LAGUNA experiment. In fact from fig.8 and observing the LAGUNA contours, the two top panels tell us that for normal hierarchy $0.05 \lesssim P_{\mu e} \lesssim 0.14$, $0.37 \lesssim P_{\mu\mu} \lesssim 0.40$, while for inverse hierarchy $0.02 \lesssim P_{\mu e} \lesssim 0.22$, $0.032 \lesssim P_{\mu\mu} \lesssim 0.073$. Similarly from the middle panels in normal hierarchy $0.01 \lesssim P_{\bar{\mu}e} \lesssim 0.21$, $0.36 \lesssim P_{\bar{\mu}\bar{\mu}} \lesssim 0.50$ while in inverse hierarchy $0.02 \lesssim P_{\bar{\mu}e} \lesssim 0.16$, $0.03 \lesssim P_{\bar{\mu}\bar{\mu}} \lesssim 0.06$. Thus it follows that the best possibilities for hierarchy distinction lie on the investigation of channels $\mu\mu$ and $\bar{\mu}\bar{\mu}$ at an energy near 0.5 GeV in the LAGUNA experiment. In fact in all cases a dedicated observation of fig.8 shows that the difference between the probabilities for normal and inverse hierarchies is substantial

$$P_{\mu\mu}(NH) - P_{\mu\mu}(IH) \geq 0.30 \quad P_{\bar{\mu}\bar{\mu}}(NH) - P_{\bar{\mu}\bar{\mu}}(IH) \geq 0.32 \quad (22)$$

and moreover it is also seen that the other two experiments (*No ν a* and LBNE) cannot offer such a possibility. Since this is the most favourable case for hierarchy determination, we have also evaluated this probability difference using the second octant solution for θ_{23} (eq.(16)). The result is

$$P_{\mu\mu}(NH) - P_{\mu\mu}(IH) \geq 0.30 \quad P_{\bar{\mu}\bar{\mu}}(NH) - P_{\bar{\mu}\bar{\mu}}(IH) \geq 0.29 \quad (23)$$

Furthermore if the hierarchy is normal, inspection of the bottom left panel of fig.8 shows that there are realistic prospects for δ_{CP} evaluation. In fact for LAGUNA, whose contour appears in this scale similar to a circle, and for the μe channel, we have $0.05 \lesssim P_{\mu e} \lesssim 0.14$. In most of this interval, namely $0.06 \lesssim P_{\mu e} \lesssim 0.13$, the two possible values of $P_{\bar{\mu}\bar{e}}$ are reasonably apart from each other: either $P_{\bar{\mu}\bar{e}} \lesssim 0.04$ or $0.17 \lesssim P_{\bar{\mu}\bar{e}} \lesssim 0.21$. In this way the ambiguity in δ_{CP} can possibly be lifted. If otherwise $P_{\mu e}$ is found to lie close to either end of the interval, namely 0.05 or 0.14, the value of δ_{CP} is also unambiguously determined, as there is only one possibility in each case: $\delta_{CP} \sim 135^\circ$ or $\delta_{CP} \sim 315^\circ$ respectively. So far all results obtained are for the θ_{23} first octant solution (eq.(15)). Still for the energy value being considered now ($E=0.5$ GeV) we show in fig.9 the same as fig.8 for the second octant solution ($\theta_{23} > 45^\circ$, eq.(16)) whose results are similar. For larger energies the distinction between the first and second octant solutions is even less clear as all contours pertaining to the three experiments become closer. We will return to this point in the next section.

810 km		
Channel	E (GeV)	P
$\mu\mu$	8.9 – 9.1	0.93 – 0.94
$\bar{\mu}\bar{e}$	11.6 – 12.4	$(1.75 - 2.0) \times 10^{-3}$
$\bar{\mu}\bar{\mu}$	8.8 – 12.4	0.93 – 0.96

Table 1: *The energy and oscillation probability for a magic baseline in normal hierarchy at Nova (810 km): for each oscillation channel and the neutrino energy range the probability shown is nearly independent of δ_{CP} . No magic baseline is found to exist for LBNE and LAGUNA in the energy range $[0.5, 12]$ GeV in normal hierarchy.*

810 km			2290 km	
Channel	E (GeV)	P	E (GeV)	P
μe	11.8 – 12.4	$(1.1 - 1.2) \times 10^{-3}$	—	—
$\mu\mu$	8.9 – 12.3	0.93 – 0.96	—	—
$\bar{\mu}\bar{\mu}$	8.8 – 8.9	0.92 – 0.93	4.7 – 5.0	$(7.0 - 9.0) \times 10^{-2}$

Table 2: *The same as table 1 in inverse hierarchy for Nova (810 km) and LAGUNA (2290 km). No magic baseline is found to exist for LBNE in the energy range $[0.5, 12]$ GeV in inverse hierarchy.*

Finally given the source-detector distances for Nova, LBNE and LAGUNA, we have estimated the necessary neutrino energy for each distance to become a magic baseline and the corresponding oscillation probability. We analysed the energy interval $[0.5, 12]$ GeV for which all three detectors are designed. Our results are shown in tables 1 and 2. For each oscillation channel we show the energy range where the probability is nearly constant with

detectors located at 810 km from the neutrino source (Nova) and 2290 km (LAGUNA). For LBNE no magic baseline is found to exist in this energy range. We note that for the $\bar{\mu}\bar{\mu}$ channel both distances can become magic baselines, whereas for μe with normal and $\bar{\mu}\bar{e}$ with inverse hierarchy none of the distances is suitable. Since at the magic baseline the oscillation probability becomes δ_{CP} independent, any significant deviation from the oscillation prediction will be the signature of nonstandard interactions [46], [47], [48].

4 T2K and Nova

The main objective of the T2K experiment [12] is to discover ν_e appearance from ν_μ . The collaboration reported their first results in June 2011 [49] which were later improved [50] and also reported evidence for ν_μ disappearance [51]. The experiment is a long baseline off-axis one with a 295 km source-detector distance from Tokai (J-PARC) to Kamioka (SuperKamiokande) and its peak neutrino energy is around 600 MeV.

Our aim in this section is twofold: to obtain the predictions for the oscillation probabilities $P_{\mu e}$ and $P_{\mu\mu}$ at T2K displaying them in terms of biprobability plots and to explore the possible complementarity between T2K and Nova. Our results are shown in the four panels of fig.10. We consider normal and inverse hierarchies (left and right panels) and first and second octant solutions for θ_{23} (top and bottom panels).

We recall that in the previous section the prospective data from one experiment were compared at the same energy for different hierarchies and/or different octants. In no case the contours from two different experiments were ever directly compared. Thus it was ensured that the comparisons were made at the same point in the oscillation phase. Exploring the complementarity between T2K and Nova, since the two experiments operate at different phases, requires a reduction of the probability to the same phase. Given the fact that T2K runs with a peak neutrino energy $E=0.6$ GeV at 295 km distance one must operate Nova, whose source-detector distance is 810 km, at a neutrino energy value satisfying

$$\left(\frac{L}{E}\right)_{Nova} = \left(\frac{L}{E}\right)_{T2K} \quad (24)$$

which gives $E_{Nova} \simeq 1.65$ GeV. In fig.10 the dotted contours refer to T2K ($E=0.6$ GeV) and the full contours to Nova ($E=1.65$ GeV). Hence observing the left and right panels of fig.10 on each row, it is seen that

$$(P_{\mu e})_{Nova} > (P_{\mu e})_{T2K} \quad (\text{normal hierarchy}) \quad (P_{\mu e})_{Nova} < (P_{\mu e})_{T2K} \quad (\text{inverse hierarchy}) .$$

On the other hand observing the top and bottom panels on each column,

$$(P_{\mu\mu})_{Nova} > (P_{\mu\mu})_{T2K} \quad (\theta_{23} < 45^\circ) \quad (P_{\mu\mu})_{Nova} < (P_{\mu\mu})_{T2K} \quad (\theta_{23} > 45^\circ) .$$

Although these inequalities apply for any value of δ_{CP} , the differences in the probabilities are so small that the possibility of ever detecting them in this way is slim.

5 Summary and conclusions

We have investigated the prospects for distinguishing normal from inverse neutrino mass hierarchies, δ_{CP} determination and first vs. second octant θ_{23} solutions with T2K, *Nova*, LBNE and LAGUNA long baseline experiments. We examined the oscillation channels which are possibly relevant for these, namely μe , $\mu\mu$ and their antineutrino counterparts. Owing to the baseline distances involved, the neutrinos are assumed to pass through the Earth's mantle only. The starting point for our numerical analysis is the general formula for the matter oscillation probability derived in section 2. The discrepancies between the results from the leading term approximations existing in the literature based on the smallness of the mass square differences ratio or the θ_{13} mixing angle were also examined.

The main results of our paper are described in section 3.2 and displayed in fig.8. They are suggestive of the importance of LAGUNA and its operation at a neutrino energy around 0.5 GeV. Otherwise we have found that there are also good possibilities to distinguish between hierarchies with other experiments provided the neutrino energy can be tuned to reasonable accuracy. To this end the oscillation channels which can provide the best information are the muon and antimuon disappearance ones, namely $\nu_\mu \rightarrow \nu_\mu$ and $\bar{\nu}_\mu \rightarrow \bar{\nu}_\mu$. For a neutrino energy $E \simeq 1$ GeV the LBNE far detector will be confronted with a probability $P_{\bar{\mu}\bar{\mu}} \simeq 0.48$ for inverse or a probability $0.62 \lesssim P_{\bar{\mu}\bar{\mu}} \lesssim 0.66$ for normal hierarchy (see fig.3, bottom panels), whereas for *Nova* these are $0.65 \lesssim P_{\bar{\mu}\bar{\mu}} \lesssim 0.68$ (inverse) and $0.55 \lesssim P_{\bar{\mu}\bar{\mu}} \lesssim 0.56$ (normal) as can also be seen from fig.3 (top panels). On the other hand for a neutrino energy $E \simeq 0.5$ GeV the possibility of hierarchy differentiation looks much brighter. In fact if the hierarchy is inverse, for the $\mu\mu$ channel in the LAGUNA far detector one expects $0.03 \lesssim P_{\mu\mu} \lesssim 0.07$, if it is normal then $0.37 \lesssim P_{\mu\mu} \lesssim 0.40$ (fig.8, top panels). Moreover for the $\bar{\mu}\bar{\mu}$ channel and for LAGUNA with inverse hierarchy we obtain $0.03 \lesssim P_{\bar{\mu}\bar{\mu}} \lesssim 0.06$ and with normal hierarchy $0.36 \lesssim P_{\bar{\mu}\bar{\mu}} \lesssim 0.50$ (fig.8, middle panels). The difference between the oscillation probabilities $P_{\bar{\mu}\bar{\mu}}$ for normal and inverse hierarchy is thus 0.32 or larger and for $P_{\mu\mu}$ it is 0.30 or larger (see eq.(22)). Hence the $\mu\mu$ and $\bar{\mu}\bar{\mu}$ channels at LAGUNA with a neutrino energy $E \simeq 0.5$ GeV seem to be the most promising ones to explore in order to find out the mass hierarchy. On the other hand the complementarity between T2K and *Nova*, presented in fig.10, does not offer a clear perspective for the mass hierarchy determination.

For the θ_{23} solution in the second octant, we have also checked the possible distinction between hierarchies. The chances look almost identical as for the first octant solution, although slightly disfavoured in the $\bar{\mu}\bar{\mu}$ channel (see eq.(23)). Distinguishing between first and second octant solutions on the other hand looks difficult as can be seen from the comparison between figs.8 and 9 and from fig.10.

As for δ_{CP} determination the LAGUNA far detector offers good chances for its feasibility on the basis of observing the μe and $\bar{\mu}\bar{e}$ channels. Again the neutrino energy must be tuned to $E \simeq 0.5$ GeV. Then if one is able to experimentally distinguish between probabilities $P_{\bar{\mu}\bar{e}} \lesssim 0.04$ and $0.17 \lesssim P_{\bar{\mu}\bar{e}} \lesssim 0.21$, a relatively narrow interval for δ_{CP} can be determined (see fig.8, bottom left panel). Again, for θ_{23} in the second octant the prospects are practically

the same.

Finally, regarding nonstandard interactions, since the baseline distances are a priori fixed, these will become magic for a conveniently chosen value of the neutrino energy. This energy was evaluated in section 3 along with the corresponding oscillation probability. Given this probability, any deviation from such a value is a signature of nonstandard interactions. In the appropriate neutrino energy interval for the three experiments, namely $[0.5, 12]$ GeV, the range to search for magic baselines is $E_\nu \geq 8.8$ GeV for *No ν a* and $(4.7 - 5.0)$ GeV for LAGUNA. No magic baseline apparently exists for LBNE in the above interval. Detailed results are shown in tables 1 and 2.

To conclude, accelerator based long baseline neutrino experiments offer good prospects to discover the δ_{CP} phase range, the mass hierarchy and may be nonstandard interactions if they really exist.

Acknowledgments

We acknowledge discussions with Evgeni Akhmedov and Luis Lavoura. C. R. Das gratefully acknowledges a scholarship from Fundação para a Ciência e a Tecnologia (FCT, Portugal) ref. SFRH/BPD/41091/2007. This work was partially supported by FCT through the projects CERN/FP/123580/2011 PTDC/FIS/ 098188/2008 and CFTP-FCT Unit 777 which are partially funded through POCTI (FEDER).

References

- [1] B. T. Cleveland, T. Daily, R. Davis, Jr., J. R. Distel, K. Lande, C. K. Lee, P. S. Wildenhain and J. Ullman, *Astrophys. J.* **496** (1998) 505.
- [2] T. A. Kirsten [GNO Collaboration], *Nucl. Phys. Proc. Suppl.* **118** (2003) 33.
- [3] J. N. Abdurashitov *et al.* [SAGE Collaboration], *J. Exp. Theor. Phys.* **95** (2002) 181 [*Zh. Eksp. Teor. Fiz.* **122** (2002) 211] [astro-ph/0204245].
- [4] K. Abe *et al.* [Super-Kamiokande Collaboration], *Phys. Rev. D* **83** (2011) 052010 [arXiv:1010.0118 [hep-ex]].
- [5] B. Aharmim *et al.* [SNO Collaboration], *Phys. Rev. C* **72** (2005) 055502 [nucl-ex/0502021].
- [6] G. Bellini *et al.* [Borexino Collaboration], *Phys. Rev. D* **82** (2010) 033006 [arXiv:0808.2868 [astro-ph]].
- [7] B. Aharmim *et al.* [SNO Collaboration], *Phys. Rev. Lett.* **101** (2008) 111301 [arXiv:0806.0989 [nucl-ex]].

- [8] R. Wendell *et al.* [Super-Kamiokande Collaboration], Phys. Rev. D **81** (2010) 092004 [arXiv:1002.3471 [hep-ex]].
- [9] S. J. Parke, FERMILAB-CONF-93-056-T, C93-01-30 Presented at Conference: C93-01-30 (Moriond 1993:Part.Phys.:0229-236), hep-ph/9304271.
- [10] B. C. Barish, Nucl. Phys. Proc. Suppl. **70** (1999) 227.
- [11] P. Adamson *et al.* [MINOS Collaboration], Phys. Rev. Lett. **108** (2012) 191801 [arXiv:1202.2772 [hep-ex]].
- [12] K. Abe *et al.* [T2K Collaboration], Nucl. Instrum. Meth. A **659** (2011) 106 [arXiv:1106.1238 [physics.ins-det]].
- [13] R. Patterson The NO ν A Experiment: Status and Outlook, Talk given at the Neutrino 2012 Conference, June 3-9, 2012, Kyoto, Japan, <http://neu2012.kek.jp/>.
- [14] C. Sirignano [OPERA Collaboration], Nucl. Phys. Proc. Suppl. **221** (2011) 268.
- [15] G. J. Feldman, J. Hartnell and T. Kobayashi, arXiv:1210.1778 [hep-ex].
- [16] F. P. An *et al.* [DAYA-BAY Collaboration], Phys. Rev. Lett. **108** (2012) 171803 [arXiv:1203.1669 [hep-ex]].
- [17] J. K. Ahn *et al.* [RENO Collaboration], Phys. Rev. Lett. **108** (2012) 191802 [arXiv:1204.0626 [hep-ex]].
- [18] Y. Abe *et al.* [DOUBLE-CHOOZ Collaboration], Phys. Rev. Lett. **108** (2012) 131801 [arXiv:1112.6353 [hep-ex]].
- [19] http://www.fnal.gov/directorate/lbne_reconfiguration/index.shtml
- [20] C. H. Albright *et al.* [Neutrino Factory/Muon Collider Collaboration], physics/0411123.
- [21] <http://beta-beam.web.cern.ch/beta-beam/various/reference.htm>
- [22] V. Barger, D. Marfatia and K. Whisnant, Phys. Rev. D **65** (2002) 073023 [hep-ph/0112119].
- [23] J. Burguet-Castell, M. B. Gavela, J. J. Gomez-Cadenas, P. Hernandez and O. Mena, Nucl. Phys. B **608** (2001) 301 [hep-ph/0103258].
- [24] H. Minakata, H. Nunokawa and S. J. Parke, Phys. Rev. D **66** (2002) 093012 [hep-ph/0208163].
- [25] M. Ishitsuka, T. Kajita, H. Minakata and H. Nunokawa, Phys. Rev. D **72** (2005) 033003 [hep-ph/0504026].

- [26] S. Bertolucci, A. Blondel, A. Cervera, A. Donini, M. Dracos, D. Duchesneau, F. Dufour and R. Edgecock *et al.*, arXiv:1208.0512 [hep-ex].
- [27] B. Richter, hep-ph/0008222.
- [28] S. Geer, Phys. Rev. D **57** (1998) 6989 [Erratum-ibid. D **59** (1999) 039903] [hep-ph/9712290].
- [29] D. Ayres *et al.* [Neutrino Factory and Muon Collider Collaboration], physics/9911009 [physics.acc-ph].
- [30] C. R. Prior, Proceedings of PAC09, Vancouver, BC, Canada, p.2739, PAC09-WE6PFP099.
- [31] J. Burguet-Castell, M. B. Gavela, J. J. Gomez-Cadenas, P. Hernandez and O. Mena, Nucl. Phys. B **646** (2002) 301 [hep-ph/0207080].
- [32] O. Mena and S. J. Parke, Phys. Rev. D **70** (2004) 093011 [hep-ph/0408070].
- [33] H. Nunokawa, S. J. Parke and R. Zukanovich Funchal, Phys. Rev. D **72** (2005) 013009 [hep-ph/0503283].
- [34] P. Huber, M. Lindner, T. Schwetz and W. Winter, JHEP **0911** (2009) 044 [arXiv:0907.1896 [hep-ph]].
- [35] L. S. Kisslinger, Int. J. Mod. Phys. E **21** (2012) 1250075 [arXiv:1108.4062 [hep-ph]].
- [36] S. K. Agarwalla, S. Prakash, S. K. Raut and S. U. Sankar, arXiv:1208.3644 [hep-ph].
- [37] W. Winter, Phys. Rev. D **78** (2008) 037101 [arXiv:0804.4000 [hep-ph]].
- [38] H. Minakata and H. Nunokawa, Phys. Lett. B **413** (1997) 369 [hep-ph/9706281].
- [39] H. Minakata and H. Nunokawa, JHEP **0110** (2001) 001 [hep-ph/0108085].
- [40] A. Cervera, A. Donini, M. B. Gavela, J. J. Gomez Cadenas, P. Hernandez, O. Mena and S. Rigolin, Nucl. Phys. B **579** (2000) 17 [Erratum-ibid. B **593** (2001) 731] [hep-ph/0002108].
- [41] E. K. Akhmedov, R. Johansson, M. Lindner, T. Ohlsson and T. Schwetz, JHEP **0404** (2004) 078 [hep-ph/0402175].
- [42] J. Beringer et al. (Particle Data Group), J. Phys. D **86** (2012) 010001.
- [43] G. L. Fogli, E. Lisi, A. Marrone, D. Montanino, A. Palazzo and A. M. Rotunno, Phys. Rev. D **86** (2012) 013012 [arXiv:1205.5254 [hep-ph]].

- [44] D. V. Forero, M. Tortola and J. W. F. Valle, Phys. Rev. D **86** (2012) 073012 [arXiv:1205.4018 [hep-ph]].
- [45] P. J. Litchfield [NOuA Collaboration], Nucl. Phys. Proc. Suppl. **145** (2005) 174.
- [46] A. M. Gago, H. Minakata, H. Nunokawa, S. Uchinami and R. Zukanovich Funchal, JHEP **1001** (2010) 049 [arXiv:0904.3360 [hep-ph]].
- [47] C. R. Das and J. Pulido, Phys. Rev. D **83** (2011) 053009 [arXiv:1007.2167 [hep-ph]].
- [48] J. A. B. Coelho, T. Kafka, W. A. Mann, J. Schneps and O. Altinok, Phys. Rev. D **86** (2012) 113015 [arXiv:1209.3757 [hep-ph]].
- [49] K. Abe *et al.* [T2K Collaboration], Phys. Rev. Lett. **107** (2011) 041801 [arXiv:1106.2822 [hep-ex]].
- [50] Ken Sakashita (KEK) for T2K collaboration 2012/July/5, ICHEP 2012.
- [51] K. Abe *et al.* [T2K Collaboration], Phys. Rev. D **85** (2012) 031103 [arXiv:1201.1386 [hep-ex]].

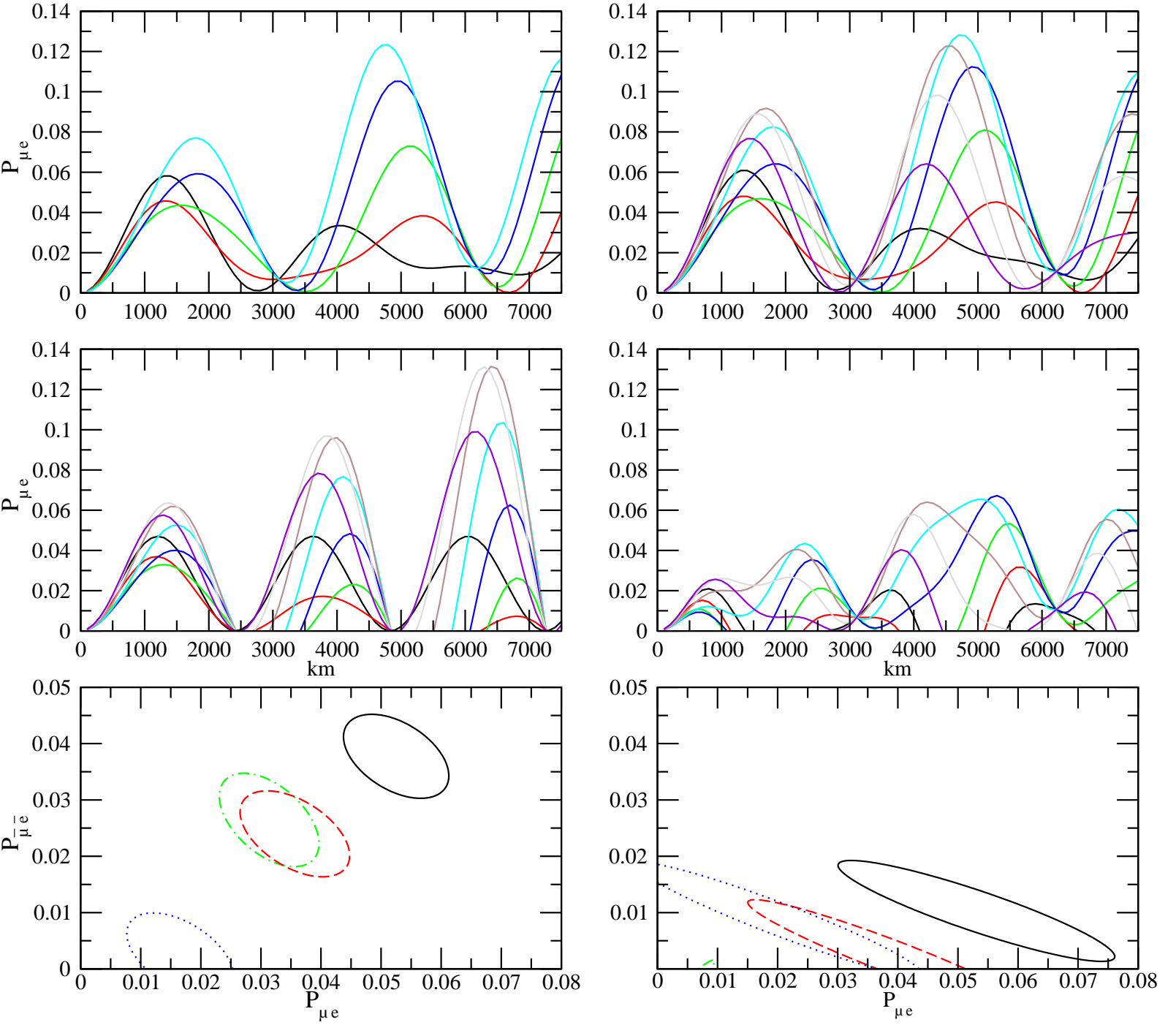


Figure 1: Four top panels (clockwise): $P_{\mu e}$ as a function of distance from 0 to 7500 km evaluated with our numerical approach, and with the approximate approximations given in [41], [40], [39] for eight values of δ_{CP} equally spaced from 0° to 360° . In our case (top left panel) constant δ_{CP} lines for 225° , 270° , 315° coincide with those for 135° , 90° , 45° . Two bottom panels: biprobability plots $P_{\mu e}, P_{\mu \bar{e}}$ at 810 km (left) and 2290 km (right) from the neutrino source. Full, dotted, dashed and dot-dashed contours are obtained from our approach, and from the approximate expressions in refs. [41], [40], [39]. All results are for θ_{23} in the first octant (eq.(15)), normal hierarchy and neutrino energy 2.3 GeV.

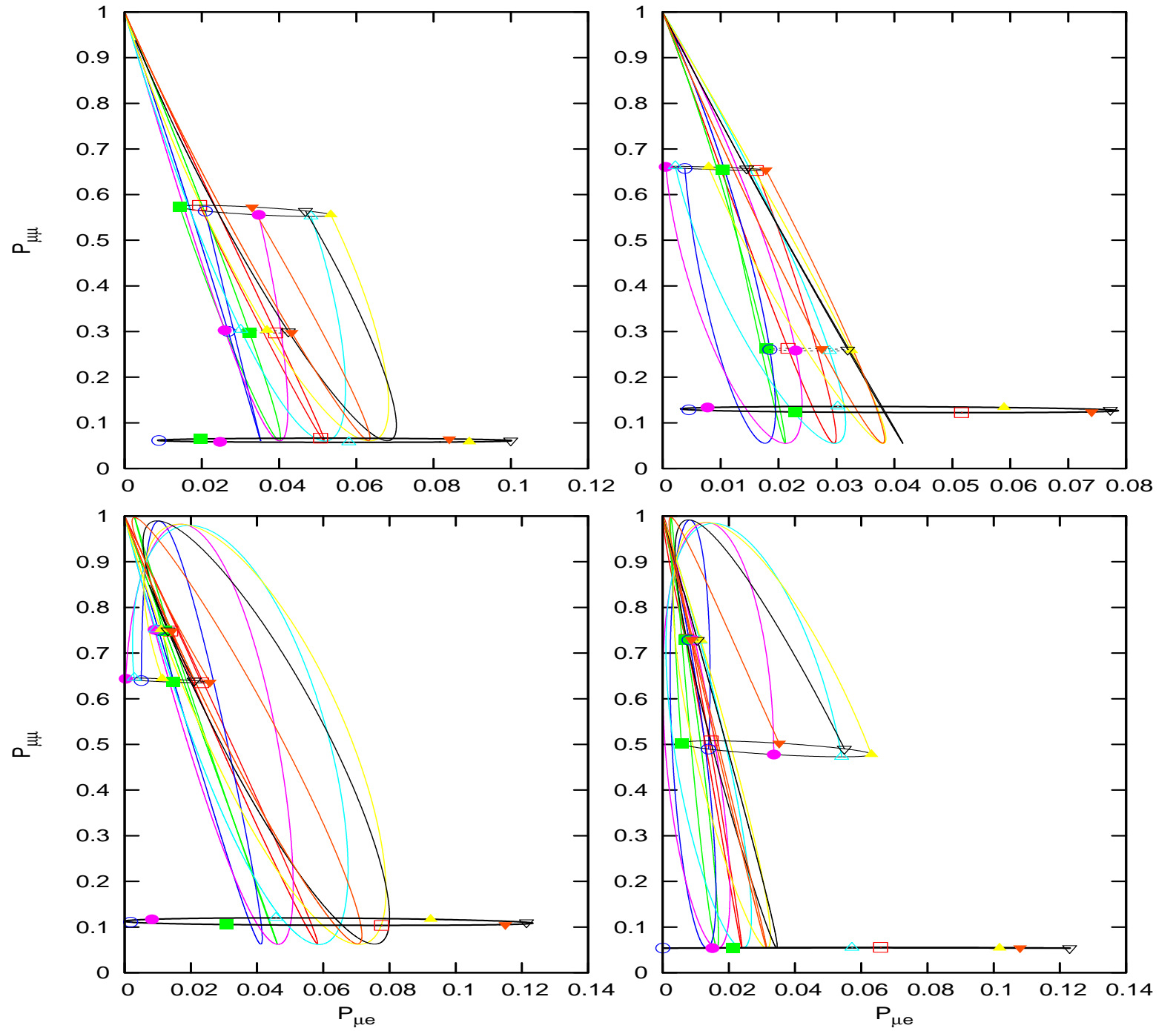


Figure 2: Biprobability plots for the $(\mu e, \mu\mu)$ channel pair with energy in the range $[0.5, 100]$ GeV and $\theta_{23} < 45^\circ$ (eq.(15)) showing the constant δ_{CP} curves (which merge at coordinates $(0,1)$ for large energy) and the constant energy contours. Top panels: 810 km distance with (from top to bottom) 1 GeV, 2.3 GeV, 0.5 GeV contours. Bottom panels: 1290 km distance with (from top to bottom) 7 GeV, 1 GeV, 0.5 GeV contours. Left and right panels: normal and inverse hierarchy respectively. Points marked as $\square, \blacksquare, \odot, \bullet, \triangle, \blacktriangle, \nabla, \blacktriangledown$ are for $\delta_{CP} = 0^\circ, 45^\circ, 90^\circ, 135^\circ, 180^\circ, 225^\circ, 270^\circ, 315^\circ$.

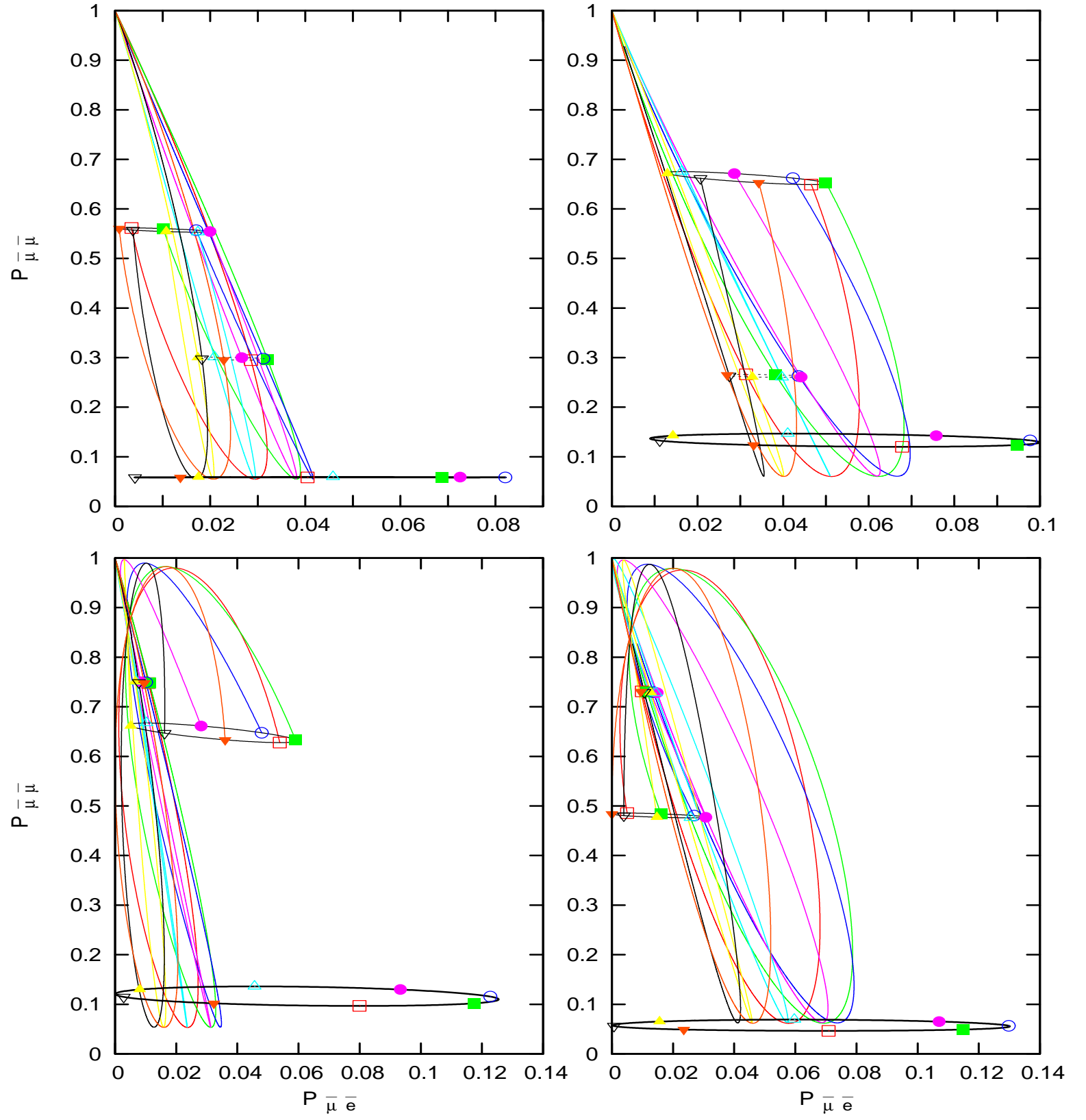


Figure 3: *The same as fig.2 for the $(\mu\bar{e}, \mu\bar{\mu})$ channel pair.*

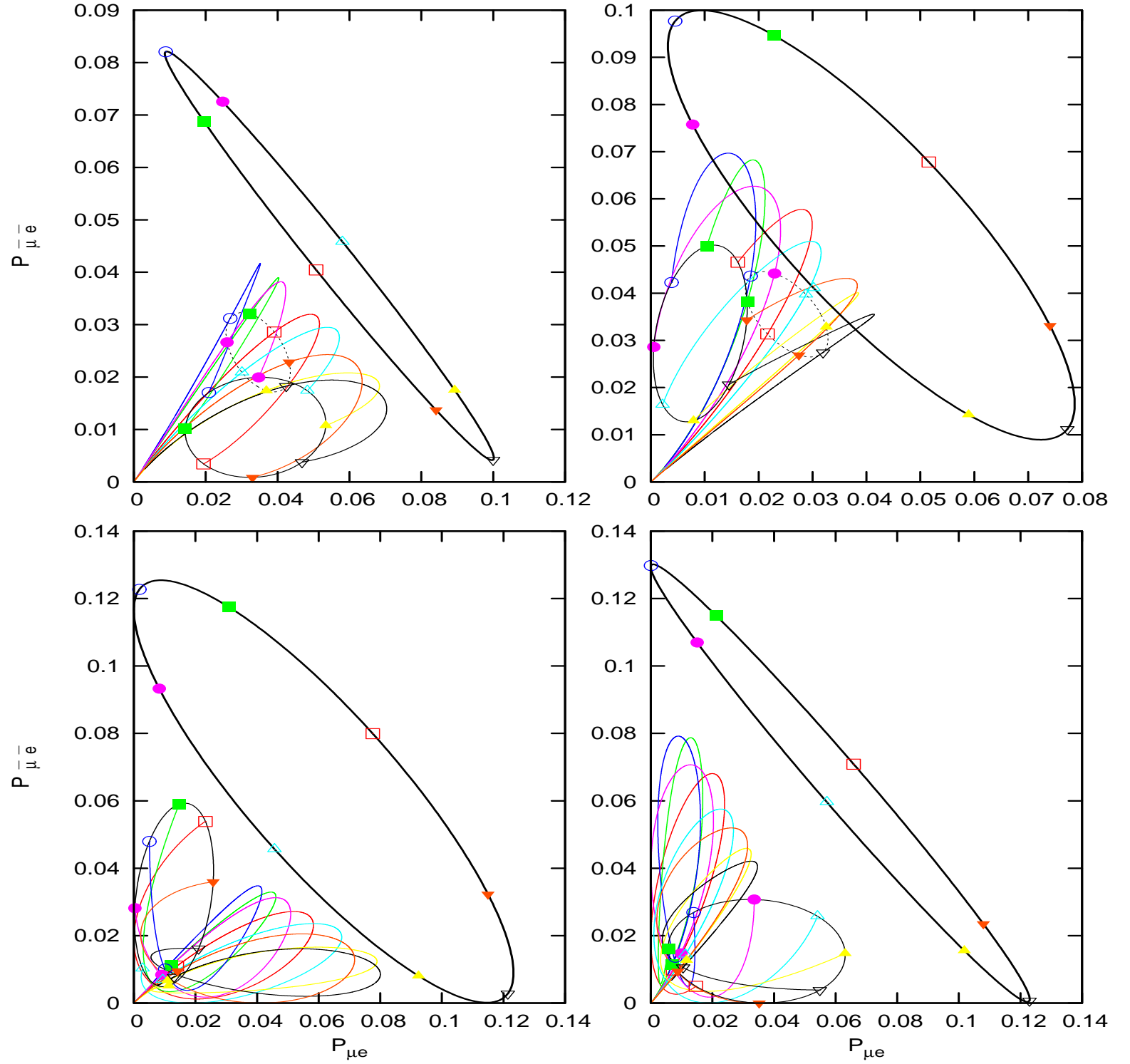


Figure 4: Biprobability plot for the $(\mu e, \bar{\mu} e)$ channel pair with energy in the range $[0.5, 100]$ GeV, $\delta_{CP} < 45^\circ$. Top panels: the contours for 810 km with 2.3 GeV (dotted), 1 GeV (thin full) 0.5 GeV (thick full). Bottom panels: the contours for 1290 km with 7 GeV (dotted), 1 GeV (thin full) 0.5 GeV (thick full). Due to the figure scale, the contour for 7 GeV in the bottom panel can hardly be seen. The constant δ_{CP} curves merge for large energy at coordinates $(0,0)$ and the values of δ_{CP} are marked as in figs.2 and 3.

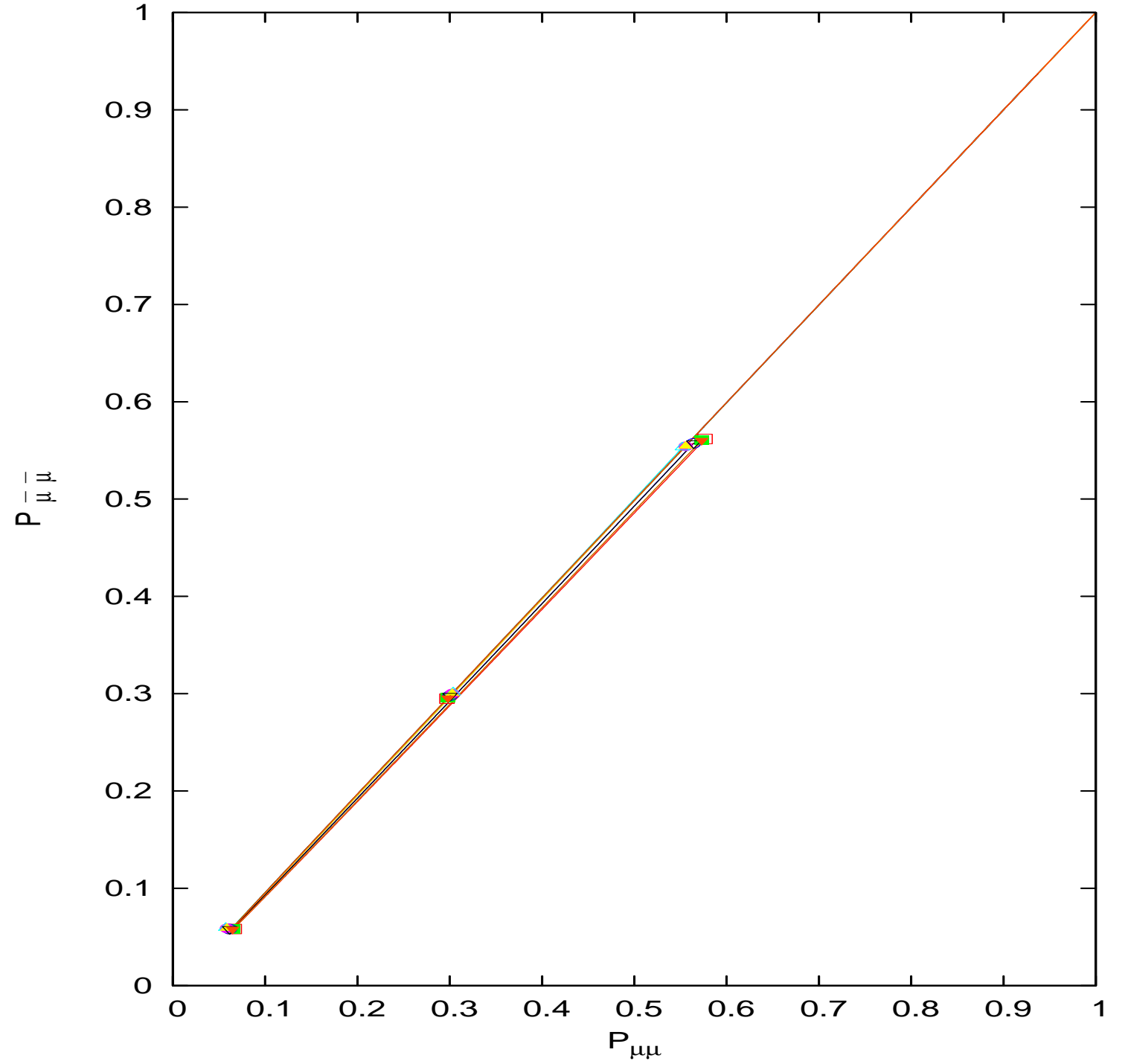


Figure 5: Biprobability curves for constant δ_{CP} for the $(\mu\mu, \bar{\mu}\bar{\mu})$ channel pair at 810 km source/detector distance in normal hierarchy with $\theta_{23} < 45^\circ$. Their intersections with the constant energy contours are marked. Their closeness prevents determination of δ_{CP} . The neutrino energy interval is $[0.5, 12]$ GeV.

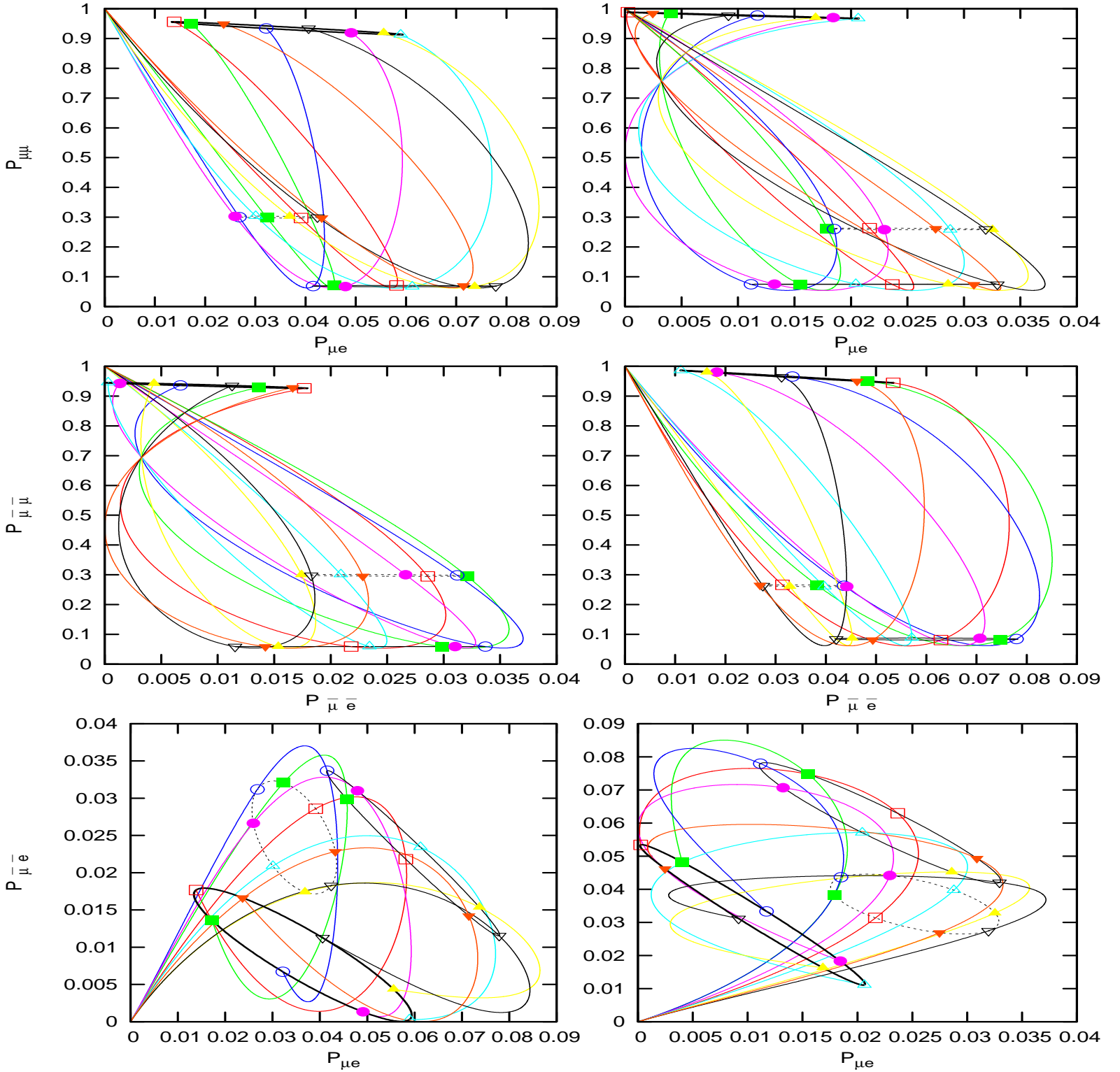


Figure 6: Biprobability graphs for neutrino energy 2.3 GeV ($\theta_{23} < 45^\circ$, eq.(15)): the curves for constant δ_{CP} for varying distance and the contours for Nova (dotted), LBNE (thin full) and LAGUNA (thick full). Left and right panels are for normal and inverse hierarchy. Top, middle and bottom panels: $(\mu e, \mu\mu)$, $(\mu e, \mu\bar{\mu})$ and $(\mu e, \bar{\mu}e)$ channel pairs. Values of δ_{CP} on each contour are marked as in fig.2: $\square, \blacksquare, \odot, \bullet, \triangle, \blacktriangle, \nabla, \blacktriangledown$ are for $\delta_{CP} = 0^\circ, 45^\circ, 90^\circ, 135^\circ, 180^\circ, 225^\circ, 270^\circ, 315^\circ$. Merging of δ_{CP} curves occurs for 0 km distance.

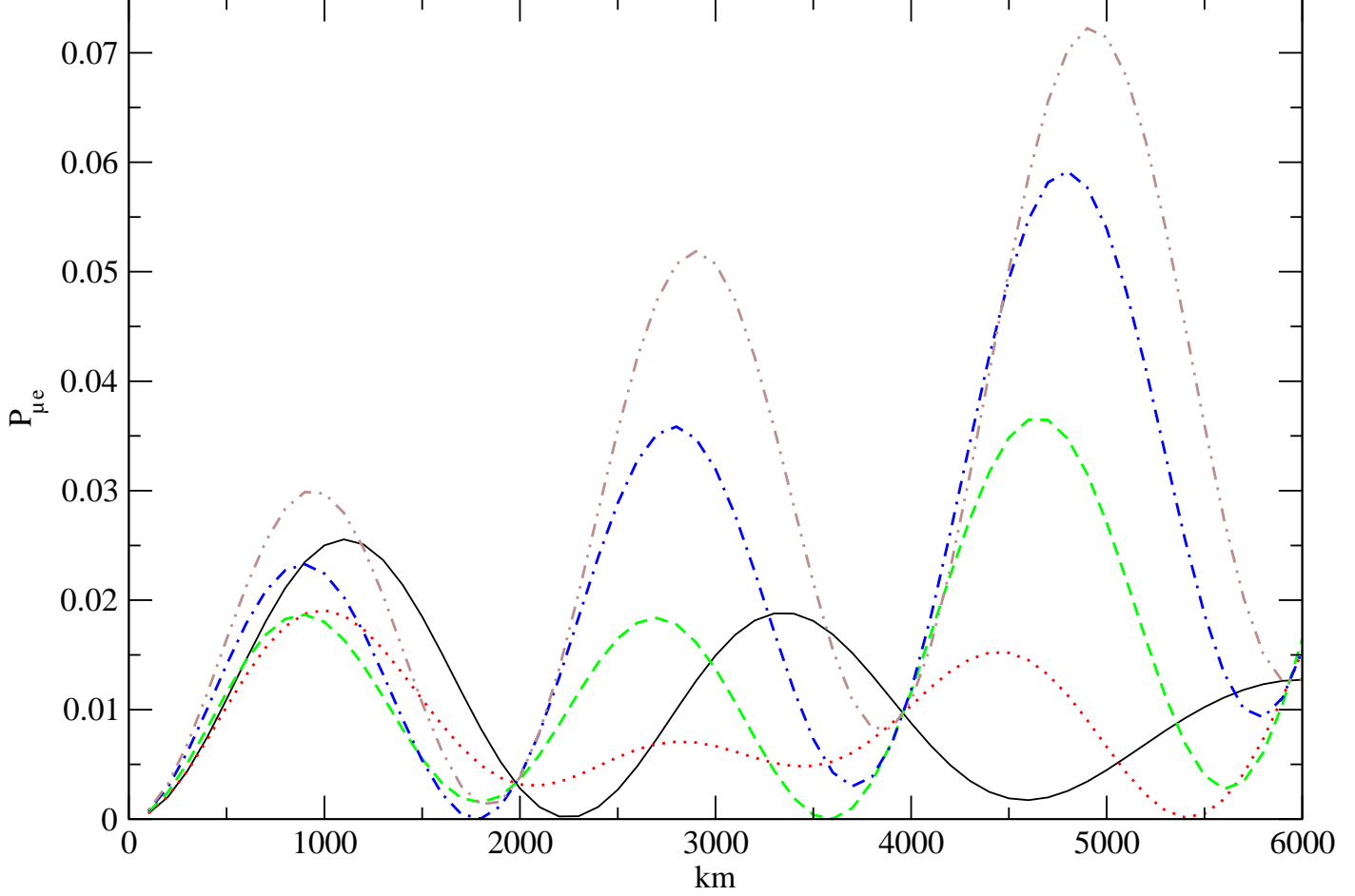


Figure 7: $P_{\mu e}$ (inverse hierarchy, $\theta_{23} < 45^\circ$, eq.(15)) as a function of distance from 0 to 6000 km for eight values of δ_{CP} equally spaced from 0° to 360° . Full, dotted, dashed, dot-dashed and dot-double dashed lines are for $\delta_{CP}=0^\circ, 45^\circ, 90^\circ, 135^\circ, 180^\circ$ respectively. $\delta_{CP}=225^\circ, 270^\circ, 315^\circ$ lines coincide with $135^\circ, 90^\circ, 45^\circ$. The neutrino energy is 2.3 GeV. The analogue of this graph for normal hierarchy is shown in the top left panel of fig.1.

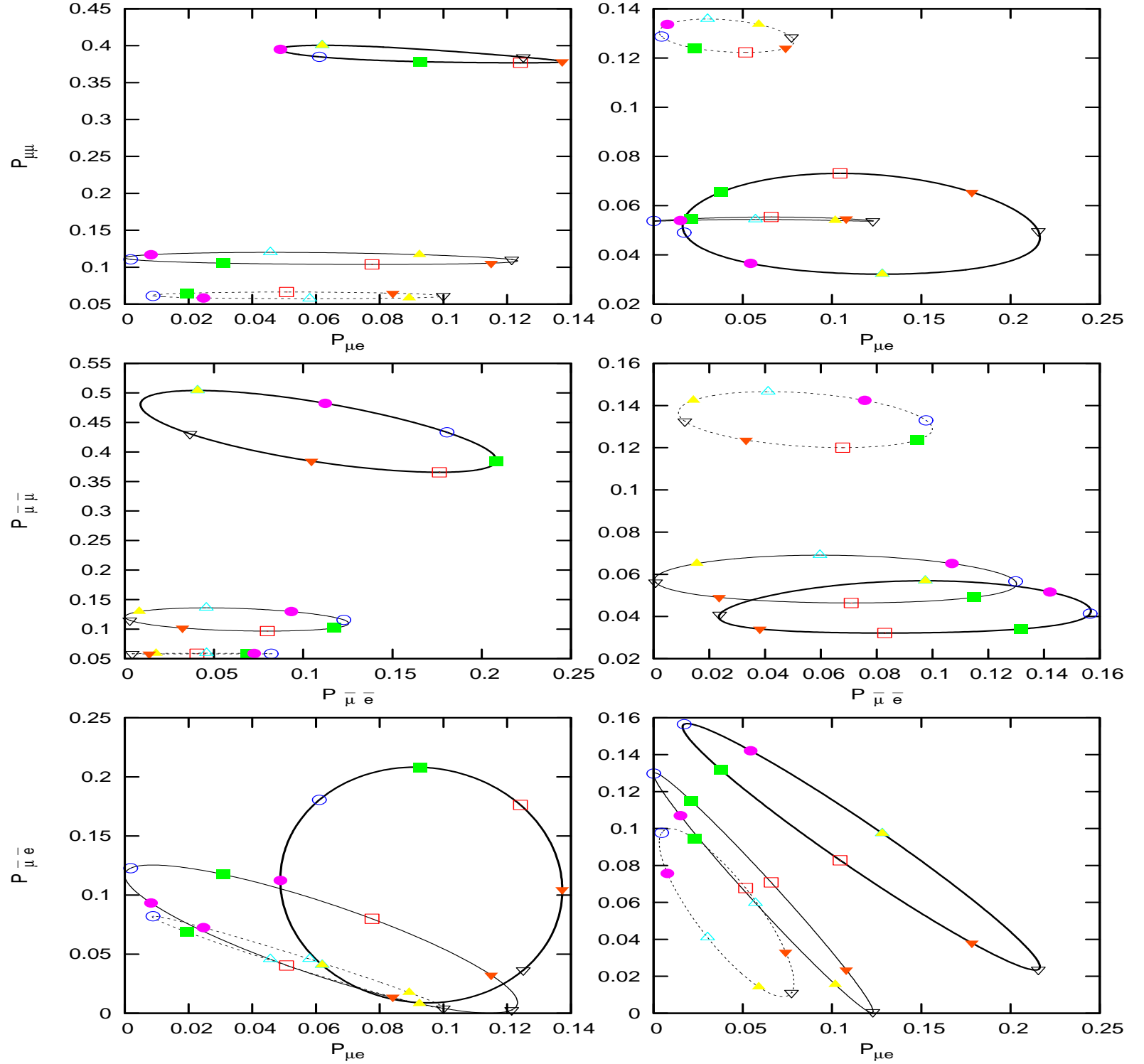


Figure 8: Biprobability graphs for neutrino energy 0.5 GeV ($\theta_{23} < 45^\circ$, eq.(15)): the contours for Nova (dotted), LBNE (dashed) and LAGUNA (full). The values of δ_{CP} on each contour are marked as in fig.2: $\square, \blacksquare, \odot, \bullet, \triangle, \blacktriangle, \nabla, \blacktriangledown$ are for $\delta_{CP} = 0^\circ, 45^\circ, 90^\circ, 135^\circ, 180^\circ, 225^\circ, 270^\circ, 315^\circ$. Left and right panels: normal and inverse hierarchy. Top, middle and bottom panels: $(\mu e, \mu\mu)$, $(\bar{\mu}e, \bar{\mu}\bar{\mu})$ and $(\mu e, \bar{\mu}e)$ channel pairs. The determination of the mass hierarchy and δ_{CP} range appear more favourable in this case than for 2.3 GeV (fig.6).

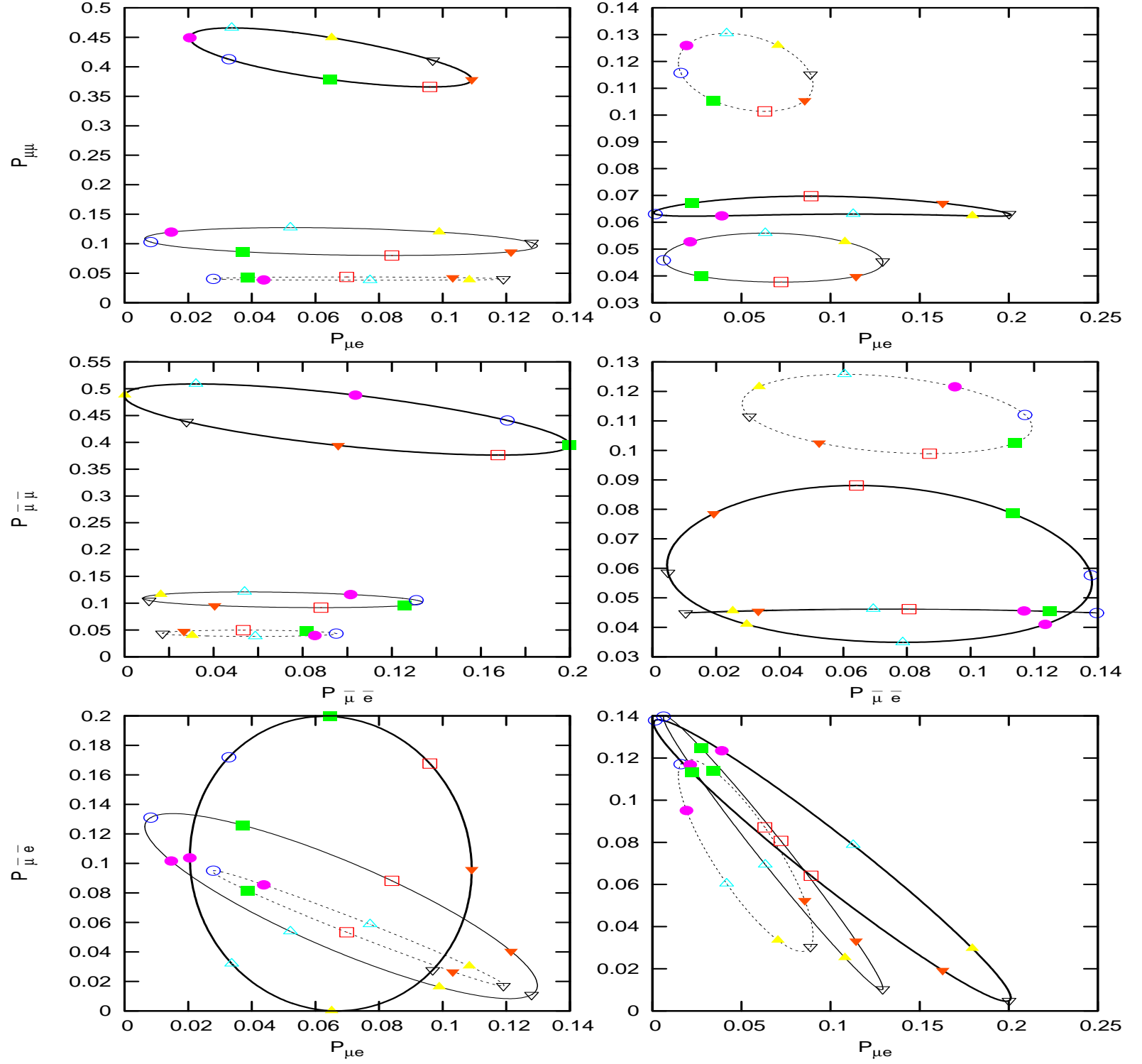


Figure 9: The same as fig.8 for the second octant solution ($\theta_{23} > 45^\circ$, eq.(16)). From comparison with fig.8 it is seen that hardly any distinction can be made between the two solutions.

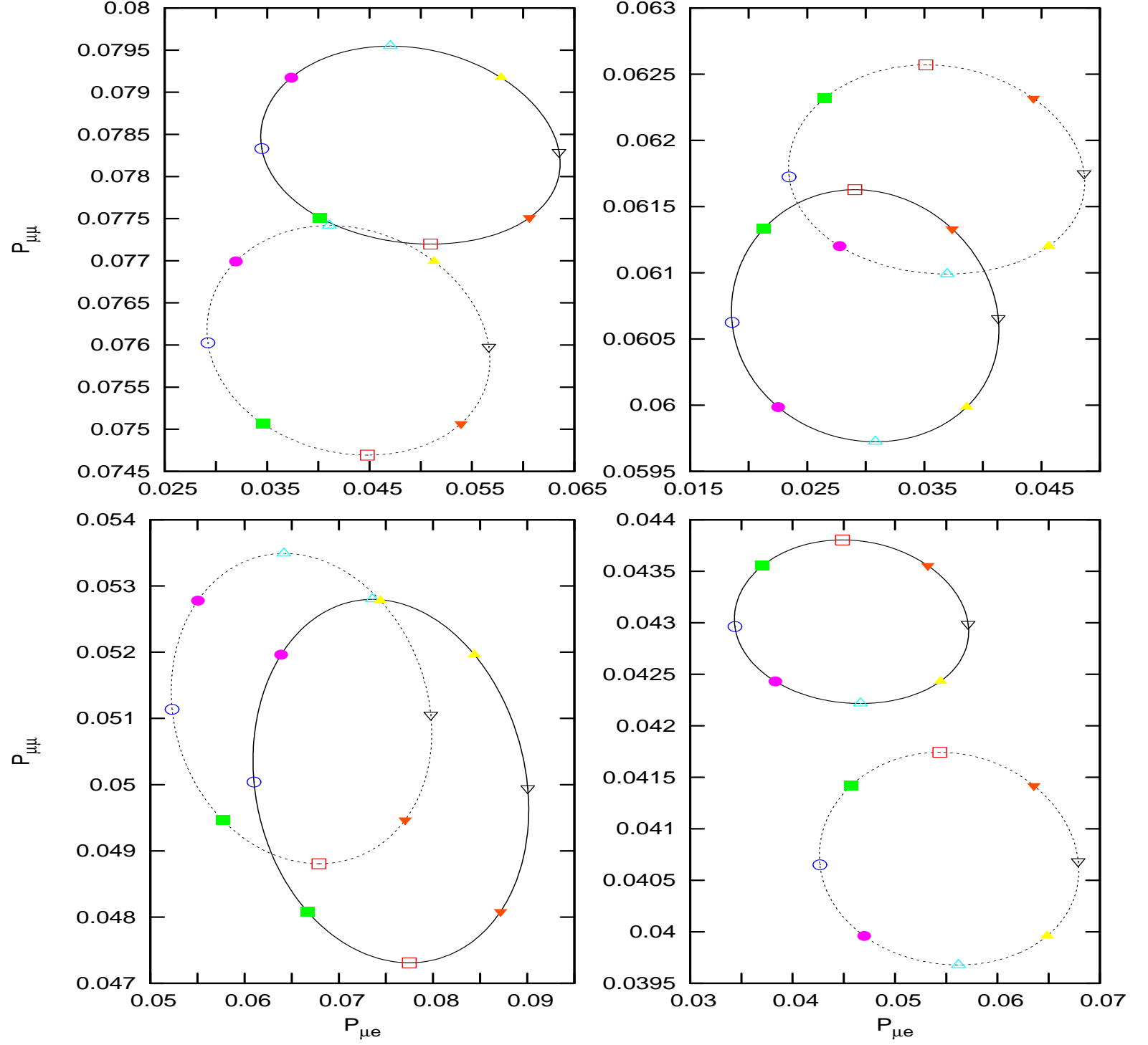


Figure 10: Comparison between T2K and Nova: left and right panels are for normal and inverse hierarchy, top and bottom ones for θ_{23} in the first (eq.(15)) and second octant (eq.(16)). Dotted contours are for T2K and full contours for Nova. Values of δ_{CP} are marked in each contour and follow the conventions of the previous figures.